

## SYNTHESIS AND CHARACTERIZATION OF CHITOSAN BASED GRAPHENE OXIDE BIONANOCOMPOSITE

Aung Than Htwe<sup>1</sup>, Naing Min Tun<sup>2</sup>, Myo Min Soe<sup>2</sup>, Masao Gohdo<sup>3</sup>, Yoichi Yoshida<sup>4</sup>, Ni Ni Than<sup>5\*</sup>

### Abstract

Nowadays, several biomaterials, including natural polymers, are used to solve and reduce the global problem of water pollution and biomedical as cellular interactions. Chitosan (CS) is one of the most studied biocompatible natural polymers. Graphene oxide (GO) is carbon-based nanomaterial capable of imparting desired properties to the scaffolds. In the present study an ecofriendly approach led to the development of biodegradable chitosan based graphene oxide bionanocomposites which have been prepared by the mixing aqueous solution of chitosan and graphene oxide. The synthesized GO and CSGO were characterized by using fourier transform infrared spectroscopy (FT IR), thermogravimetric/differential thermal analysis (TG-DTA), X-ray diffraction (XRD), field emission scanning electron microscope (FE-SEM), UV-Vis spectroscopy. Finally, the synthesized nanoparticles size and surface charge were measured by dynamic light scattering (DLS) and zeta potential analyzer, respectively. The results obtained from those different studies revealed that chitosan and graphene oxide could mix with each other homogeneously. Hence, chitosan based graphene oxide bionanocomposite were successfully synthesized and characterized.

**Keywords:** chitosan, graphene oxide, bionanocomposite, dynamic light scattering

### Introduction

Chitosan (CS), produced from chitin by deacetylation, is an environmentally friendly and renewable natural biopolymer with outstanding properties of non-toxic, biocompatible and biodegradable. Additionally, many amino and hydroxyl groups make CS absorb anionic organic compounds and metal ions efficiently by electrostatic interactions or chelating, which was widely applied in industrial, environment and biomedicine fields (Wu *et al.*, 2020). Chitosan, a copolymer of  $\beta$ [1,4]-linked 2-acetamido-2-deoxy-D-glucopyranose and 2-amino-2-deoxy-D-glucopyranose, is generally obtained by deacetylation of chitin, one of the most plentiful natural polymers on earth. Because of its good biocompatibility, biodegradability, and multiple functional groups, chitosan (CS) has attracted significant interest in a broad range of applications such as water treatment, membrane separation, food package, tissue engineering, and drug delivery. However, low mechanical properties of chitosan restrict its use in a wide-range application. (Yang *et al.*, 2010).

Chitosan-based nanomaterials have also been produced using different type of organic and inorganic nanoparticles. Consequently, chitosan has been modified using carbon nanotube, graphene, nanoclay, and metal nanoparticles. The modified chitosan has been reinforced in different polymers to form nanocomposite. These nanocomposites have several improved properties such as porosity, surface area, electrical conductivity, photoluminescence, tensile strength, morphology, and antibacterial and bio-properties (Kausar, 2019).

Graphene, a single layer of carbon atoms in a hexagonal lattice, has recently attracted much attention due to its novel electronic and mechanical properties. Graphene is usually prepared by the reduction of its precursor graphene oxide, a typical pseudo-two-dimensional oxygen-containing solid in bulk form, possesses functional groups including hydroxyls, epoxides, and carboxyls. Both graphene and graphene oxide papers show very high mechanical properties with well

---

<sup>1</sup> Assistant Lecturer, Department of Chemistry, University of Yangon, Myanmar

<sup>2</sup> Lecturers, Department of Chemistry, University of Yangon, Myanmar

<sup>3</sup> Assistant Professor, The Institute of Scientific and Industrial Research, Osaka University, Japan

<sup>4</sup> Professor, The Institute of Scientific and Industrial Research, Osaka University, Japan

<sup>5</sup> Professor and Head, Department of Chemistry, University of Yangon, Myanmar

biocompatibility, and they have potential application as biomaterials. The chemical groups of graphene oxide have been found to be a feasible and effective means of improving the dispersion of graphene. Additionally, functional side groups bound to the surface of graphene oxide or graphene sheets may improve the interfacial interaction between graphene oxide/graphene and the matrix similarly to that observed for functionalized carbon nanotube-based nanocomposites (Han *et al.*, 2011).

A single layer of carbon atoms constitutes the structure of graphene oxide (GO) packed in a hexagonal arrangement. This is a two-dimensional (2D) nanomaterial having excellent electronic, optical, and mechanical properties. Therefore, it has been able to draw significant interest very recently among the research communities. But strong van der Waals and  $\pi$ - $\pi$  interactions induce the graphene sheets to agglomerate in aqueous solution. This has posed an enormous problem in the preparation of graphene-based materials for various applications, and thus, an urgent modification toward resolving the issue has been required. To overcome this problem, GOs possessing multiple functional groups such as epoxides, hydroxyls, and carboxyls are prepared. GO along with all these functionalities can be easily exfoliated into monolayer sheets that are capable of forming a stable dispersion in water and in other solvents which are polar. These functional groups facilitate the functionalization through covalent or noncovalent routes. They endow the edges and surfaces of GO to give rise to gels with a higher rate of chemical reactivity having GO and provide them with ample modification potential because of the simple fabrication processes (Nath, 2018).

In the present work, the chitosan based graphene oxide bionanocomposite were prepared by the mixing aqueous solution of chitosan and graphene oxide. The synthesized GO and CSGO were characterized by using FTIR, TG-DTA, XRD, FE-SEM, UV-Vis. Finally, the synthesized nanoparticles size and surface charge were measured by DLS and zeta potential analyzer, respectively.

## Materials and Methods

Commercial chitosan from shrimp shell waste was purchased from Asian Technology Groups Co. Ltd., Local Industry, Yangon, Myanmar. Graphite was purchased from Sigma-Aldrich Co., (USA). All other chemicals used were of analytical reagent grade. In all investigations, the recommended standard methods and techniques involving both conventional and modern methods were provided.

### Preparation of Graphene Oxide (GO) Powder

Firstly, 3.0 g of graphite powder were placed in beaker and then 90:30 v/v ratio of 98 % of sulphuric acid: 68 % of nitric acid were added. During the reaction, the solution was in exothermic condition so it must be stirred in the ice-bath at 10 °C to maintain temperature while 9 g of  $\text{KMnO}_4$  was slowly added and stirred at 15 min after the temperature being controlled by the ice bath to 9 °C. The mixture was continuously stirred at 300 rpm. Afterward, the solution then was added to 150 mL of distilled water gradually while at the same time it was stirred with 300 rpm at 90 °C for 30 min to achieve neutral conditions. Hence, 30 mL of hydrogen peroxide ( $\text{H}_2\text{O}_2$  30%) was added into the solution and then stirred with 300 rpm for 1h. The resultant solution was centrifuged and the precipitate was washed with 600 mL hot distilled water. The brown paste was obtained. 100 mL of 10 % hydrochloric acid (10%) was added to the paste and stirred at 30 min. Then, the precipitate was washed with 200 mL distilled water with five times at 7000 rpm for 30 min due to acid free of mixture. The yellow-brown GO mixture was obtained. The obtained GO mixture was sonicated at 2 h and then was centrifuge at 3000 rpm for 30 min. The decant mixture was decanted.

The decanted was centrifuged. The GO dispersed mixture was decanted and dried in oven at 80 °C to obtain GO.

### Preparation of Chitosan/Graphene Oxide Bionanocomposite

A 1 g of chitosan was dissolved into 100 mL of 1 % aqueous acetic acid to prepare 1 % (v/v) chitosan (CS) solution. An aqueous dispersion of GO (0.1, 0.2, 0.3, 0.4, 0.5 g) in 50 mL of 1% (v/v) acetic acid was mixed with 50 mL of 1 % CS solution and sonicated for 1 h. The mixture was stirred continuously at 60 °C for 2 h, after which 0.2 mL glutaraldehyde (50 % in H<sub>2</sub>O) was added dropwise with constant stirring. A black gel of CSGO solution was cast on glass plate and dried at 60 °C. The different ratios of GO in chitosan/graphene oxide nanocomposite (CSGO0.1, CSGO0.2, CSGO0.3, CSGO0.4 and CSGO0.5) were obtained.

### Characterization

The prepared bionanocomposites were characterized by FT IR spectroscopy using PerkinElmer GX instrument. The FTIR spectra were obtained in reflectance mode with a resolution of 4 cm<sup>-1</sup> over a spectra range of 500-4000 cm<sup>-1</sup>. Thermogravimetric analysis (TGA) was performed using a DTG-60H, Thermalgravimetric analyzer, Shimadzu, Japan, URC, UY with a nitrogen flow rate of 20 °C/min. The particle size distribution (PSD) of aggregates in GO and CSGO nanocomposites were measured using an optical microscope STZ-171 with Moticam U 2.0 MP, Shimadzu which captured the images. X-ray diffraction (XRD) measurements were performed using a (Rigaku, Japan) with a Cu K $\alpha$  radiation source (wavelength  $\lambda = 0.154$  nm) at a voltage of 40 kV and a current of 50 mA. The scanning rate was 3 °/min and the scanning scope of 2 $\theta$  was from 5° to 40°. The surface morphology was analysed by field- emission scanning electron microscopy (FE-SEM, Hitachi SU8000, Japan). UV-vis absorption spectra were measured on an UVmini-1240, UV-vis Spectrophotometer, Shimadzu, Japan. The particle size distribution and zeta potential of GO and CSGO nanocomposite solutions (0.01 w/v %) were measured using a Zetasizer-Nano ZS (Malvern instruments, UK). Samples were placed into a U-shaped folded capillary cell for zeta potential measurements. Each sample was measured at room temperature (25 °C) in triplicate.

## Results and Discussion

### Characterization

The CS-GO nanocomposites were successfully prepared by in situ mineralization, where in the CSGO hydrogel was first prepared using GA as a cross-linker. CS is soluble in water at acidic pH, at which amine functional groups of the molecule undergo protonation. The cross-linking treatment with GA was carried out to decrease the degree of swelling and reinforce the mechanical and chemical stability of the composite material in a wide range of solution conditions including an acidic medium.

### FT-IR spectroscopy

The FT IR spectra of the CS, GO and CSGO bionanocomposites are shown in Figure 1(a) and (b). The broad peak at 3450 cm<sup>-1</sup> and the strong absorption peak at 1650 and 1589 cm<sup>-1</sup> are characteristic of primary amine in chitosan spectrum (Figure 1 a). The broad band at 3000 – 3500 cm<sup>-1</sup> range is attributed to the OH stretching, which overlaps the NH stretching in the same region. The characteristic chitosan absorption band at 2800 – 2900 cm<sup>-1</sup> range in spectra of all films represent >CH<sub>2</sub> and –CH<sub>3</sub> aliphatic groups, respectively. The band at 1560 – 1590 cm<sup>-1</sup> range presented the –NH bending vibration. The strong peak at 1650 cm<sup>-1</sup> (amide I) is due to the

vibrations of carbonyl (C=O) groups, which is an evidence of incomplete chitosan deacetylation. A sharp peaks near 1380 and 1420  $\text{cm}^{-1}$  correspond to deformation vibrations of OH and CH groups where as the broad peak at 1080  $\text{cm}^{-1}$  is due to glycosidic bonds. In Figure 1(b), the FT IR spectrum of GO shows a peak at 3208.43  $\text{cm}^{-1}$  that is due to the O-H stretching of the -COOH group. The peak at 1716.6  $\text{cm}^{-1}$  and 1620.24  $\text{cm}^{-1}$  are characteristics of the C=O stretch of the carboxylic group on the grapheme oxide and deformations of the O-H bond in water. The intense peak occurring at 1391  $\text{cm}^{-1}$  is due to O-H deformations of C-OH groups, and the peak at 1039.99  $\text{cm}^{-1}$  represents C-O-C stretching. This implies that the sample has strong hydrophilicity. The absorption peak at 1620.24  $\text{cm}^{-1}$  can be ascribed to the presence of benzene rings (Konwar *et al.*, 2016; Yang *et al.*, 2010). The characteristic absorption peak of the CSGO nanocomposite at 2869  $\text{cm}^{-1}$  which can be assigned to the C-H asymmetric vibration due to chitosan incorporation. The new vibration band appeared at 1541.50 -1560.49  $\text{cm}^{-1}$  due to the C=O stretching whereas the carboxylic group bands at 1716.6  $\text{cm}^{-1}$  of graphene oxide disappeared (Kumar *et al.*, 2014). According to the FT IR analysis, CSGO shows that the graphene oxide interacts with chitosan through intermolecular hydrogen bonds. So the CSGO nanocomposites should be miscibility between GO and CS.

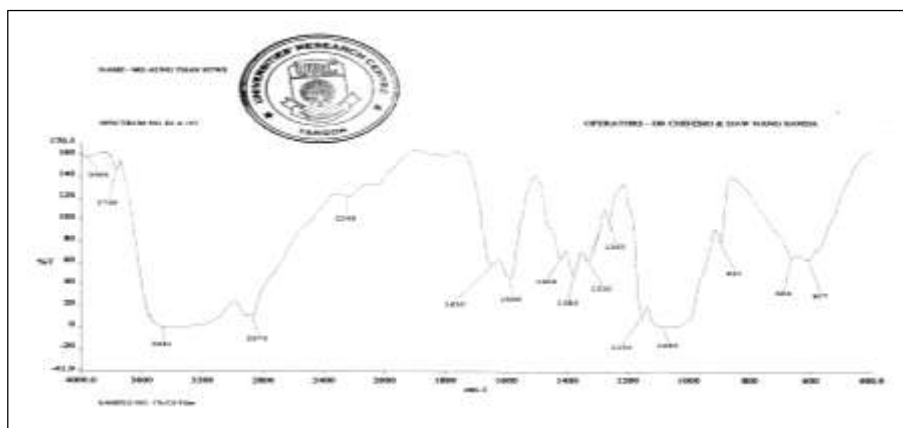


Figure 1(a). FT IR spectrum of pure CS

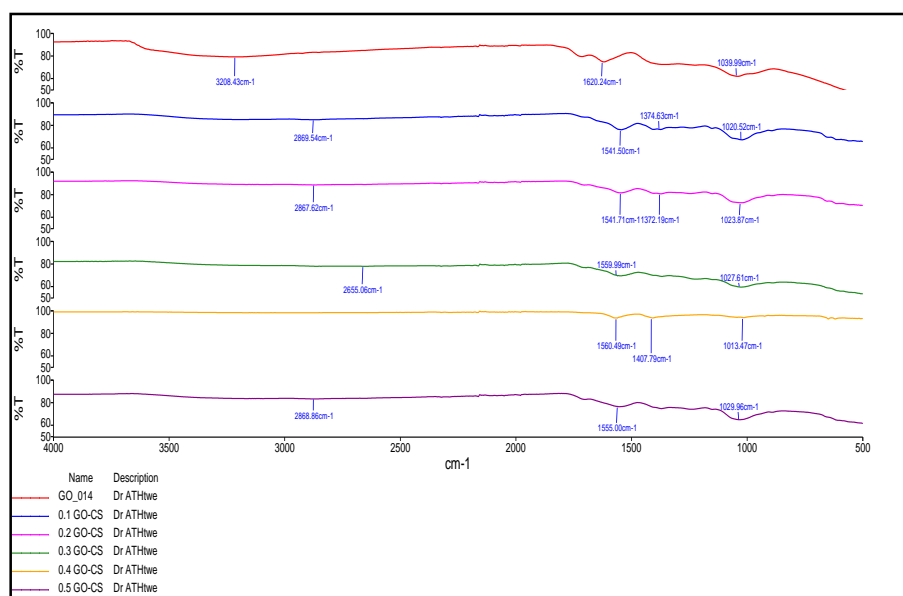


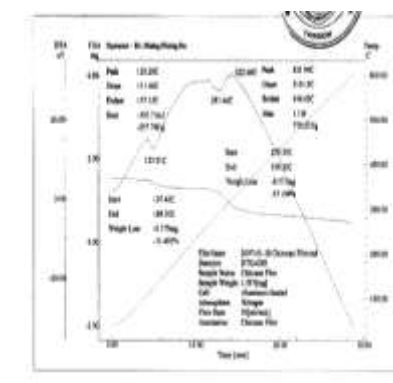
Figure 1(b). FT IR spectra of pure GO and their nanocomposites

### Thermogravimetric analysis

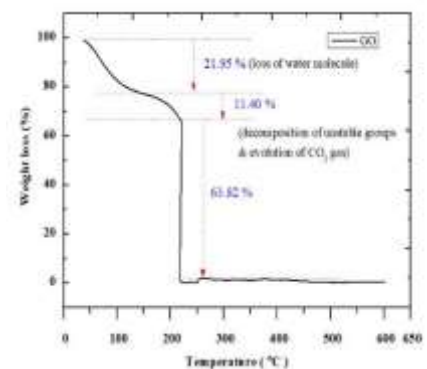
The thermal stability of the pure CS, GO and five different ratios of GO in chitosan-graphene oxide nanocomposite particles (CSGO0.1, CSGO0.2, CSGO0.3, CSGO0.4 and CSGO0.5) were studied by thermogravimetric analysis as shown in Figure 2 (a) to (g). According to the TG DTA thermogram profiles, CS showed two decomposition stages. The first stage ranges between about the temperature range is 107.43 °C to 169.30 with 11.40 % of weight loss. There is moisture evaporation upon heating. The second stage is the loss in weight 37.19 % was decomposed within the temperature range of 275.35 °C to 399.33 °C. With reference to the depolymerization and elimination of glycosidic units of CS, the decomposition at 100 °C is clearly observed. Thermal elimination of CS takes place above 200°C after the residual water gets eliminated initially around 100 °C (Aung Than Htwe, 2018).

Thermal stability of GO (Figure 2 (b)) is found to be relatively good. But around 218 °C, there is a decrease in the thermal stability. GO experienced 75.28 % weight loss at this temperature. This attributes to the thermal decomposition of unstable groups containing oxygen and evolution of CO<sub>2</sub> gas. Below 100°C, the TGA curve shows a 21.95 % weight loss, which implies the loss of water molecules bound inside the GO structure. Due to the removal of stable functional groups, mass loss occurs in the range of 250–600 °C (Nath *et al.*, 2018).

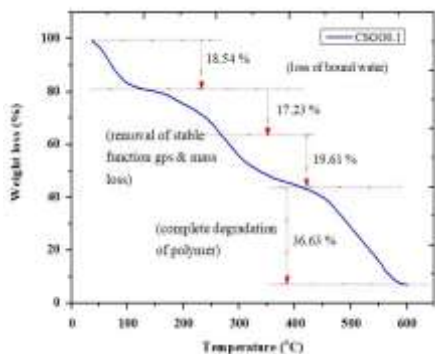
The thermogram of all CSGO shown in Figure 2(c to g), having a weight loss in three stages. The first stage ranges between about the temperature range is 36 °C to 187 °C with 18.54 % in CSGO0.1, 13.18 % in CSGO0.2, 14.79 % in CSGO0.3, 10.11 % in CSGO0.4 and 15.58 % in CSGO0.5 of weight loss. There is loss of water molecules bound inside the CSGO structure and evolution of CO<sub>2</sub>. The second stage, the temperature range between 187 °C to 365 °C was observed 36.84 % in CSGO0.1, 24.56 % in CSGO0.2, 34.75 % in CSGO0.3, 4.25 % in CSGO0.4 and 35.52 % in CSGO0.5 of weight loss. This is due to the removal of stable function groups and mass loss. The third stage is the loss in weight 36.63 % in CSGO0.1, 26.03 % in CSGO0.2, 43.34 % in CSGO0.3, 9.30 % in CSGO0.4 and 41.86 % in CSGO0.5 was observed to take place within the temperature range of 365 °C to 600 °C. In this stage, weight loss is due to complete degradation of polymer.



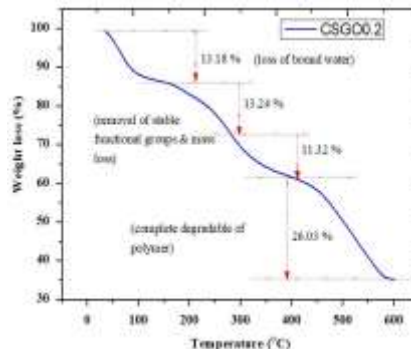
(a) CS



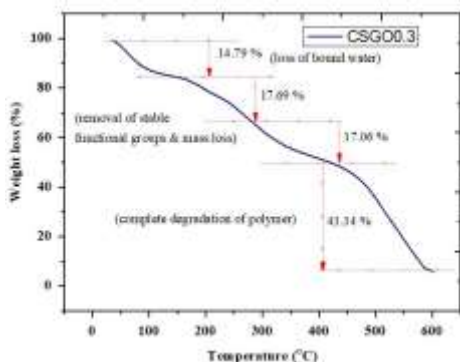
(b) GO



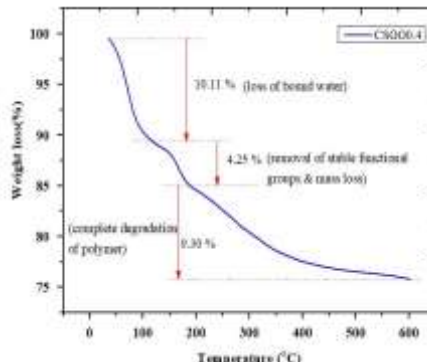
(c) CSGO0.1



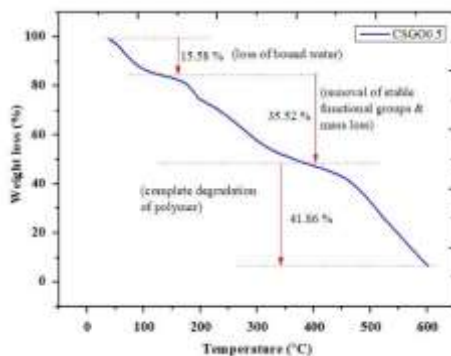
(d) CSGO0.2



(e) CSGO0.3



(f) CSGO0.4



(g) CSGO0.5

Figure 2 TG-DTA thermogram of pure and bionanocomposites

Table 1 The weight loss (%) of GO and CSGO bionanocomposite with different temperature

Temperature (°C)	Weight loss (%)					
	GO	CSGO0.1	CSGO0.2	CSGO0.3	CSGO0.4	CSGO0.5
0	100	100	100	100	100	100
100	82.72	97.21	88.29	87.36	90.3	86.86
200	71.91	75.42	83.04	79.27	84.56	74.51
300	1.23	55.72	69.53	62.73	80.38	57.76
400	1.28	44.76	61.66	51.52	77.54	47.4
500	0.33	28.79	50.34	35.49	76.53	32.67
600	0.59	7.06	35.27	6.18	75.81	6.99

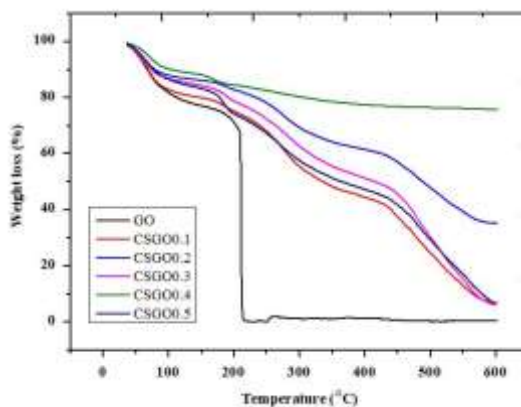


**Figure 3** TGA of GO and CSGO bionanocomposite

Compared to the original CS, the decrease in thermal stability for CS/GO hydrogel can be ascribed to the ionically formed bonds among  $\text{NH}_3^+$  and  $\text{HCOO}^-$  groups. Intermolecular hydrogen bonding interaction between amino and hydroxyl groups of CS is destroyed partly by these new ionic bonds. This change eliminates the initial crystallinity of CS, and the rigidity of the CS chains is also weakened. Compared to the TGA of original GO, the hydrogel gains improved thermal stability, which is due to the superior insulation of GO nanosheets and barrier against the mass transport of the volatile compounds generated when the polymer undergoes decay under thermal conditions (Nath *et al.*, 2018).

According to the Table 1 and Figure 3, the results demonstrated that the loading levels of the GO were low so that it can affect the decomposition temperature of the nanocomposite. It also indicates that the weight loss percent of the CSGO is relatively higher than that of GO.

### Optical microscope

Figure 4 shows the optical micrographs captured by the camera for resolution 5 mega pixel (MP) samples. In this case, 5 MP of pure GO and CSGO bionanocomposites have a higher quantity of aggregates with fewer fine particles around the large aggregates. Therefore, the image capture must be very fast. The method of measurement for particle size by optical microscopy was also useful for observing the aggregation evolution over time, specifically when fine particles agglomerate to form new, larger aggregates (Quilaqueo *et al.*, 2019).

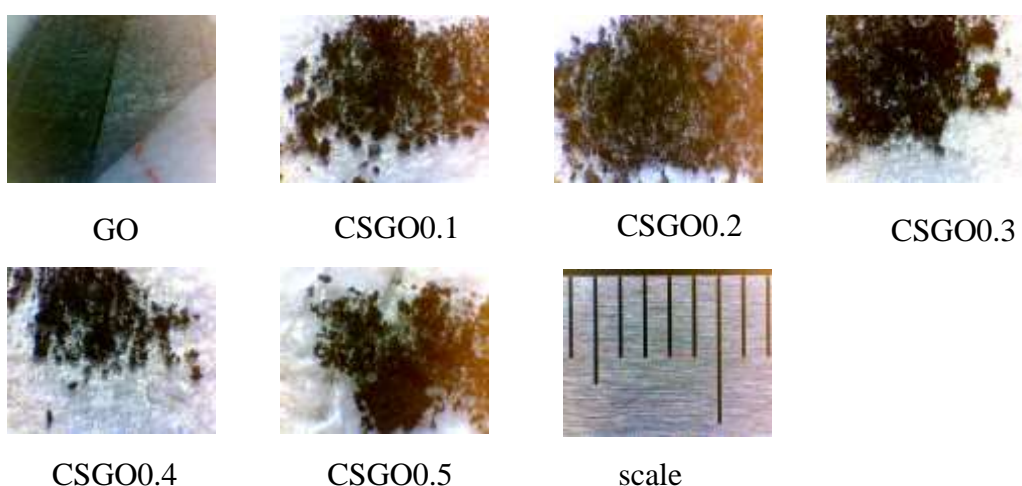


**Figure 4** Optical micrographs of pure GO and CSGO bionanocomposite

### X-ray diffraction analysis

Figure 5 represents the structural analysis of graphene oxide, chitosan and chitosan/graphene oxide bionanocomposites were investigated by X-ray diffraction. X-ray diffraction studies of graphene oxide exhibits very intense peak at  $2\theta$  is  $10.58^\circ$ . Pure chitosan films showed a characteristic peak at around  $2\theta$  is  $8.72^\circ$  and sharp peak at  $21.74^\circ$ . All of the prepared CS-GO bionanocomposite exhibit two broad peaks at  $2\theta = 9.28^\circ$  and  $21.3^\circ$  due to the generally amorphous state of the chitosan films. After the formation of CSGO nanocomposite, the intensity of all the reflections decreases. As seen in figure, it is found that the intensity of CS-GO nanocomposite peak are not only lower than GO peak but also higher than CS peak. This is because of the decrease in the degree of crystallinity of CS due to the addition of GO. Formation of new interactions between GO and CS reduces the interactions among CS chains. The peak that appears at  $2\theta = 8.09^\circ$  in the hydrogel is attributed to the increased layer spacing in the GO layers (Nath *et al.*, 2018).

The XRD pattern of the CSGO bionanocomposites shows only the CS diffraction peaks from CS and the diffraction peak of GO disappears, which clearly demonstrate the formation of fully exfoliated structure of GO sheets in the polymer matrix (Yang, 2010). When incorporation of graphene oxide in chitosan chemical structure of the chitosan films changes due to the overlap of biopolymer diffraction, it indicates that there were mainly physical interaction but scarcely chemical reaction between chitosan and graphene oxide (Han *et al.*, 2011). In this particular case, the electrostatic interaction and hydrogen bonding may contribute to a relatively ordered arrangement of the attached CS chains along the rigid template offered by GO. However, the chemical structure of the chitosan in the composites barely changes with the increasing content of graphene oxide, indicating that there were mainly physical interaction but scarcely chemical reaction between chitosan and graphene oxide (Bissessur *et al.*, 2006 and Han *et al.*, 2011). The CSGO bionanocomposite exhibited a combination of amorphous and crystalline peaks (Kumara *et al.*, 2014).

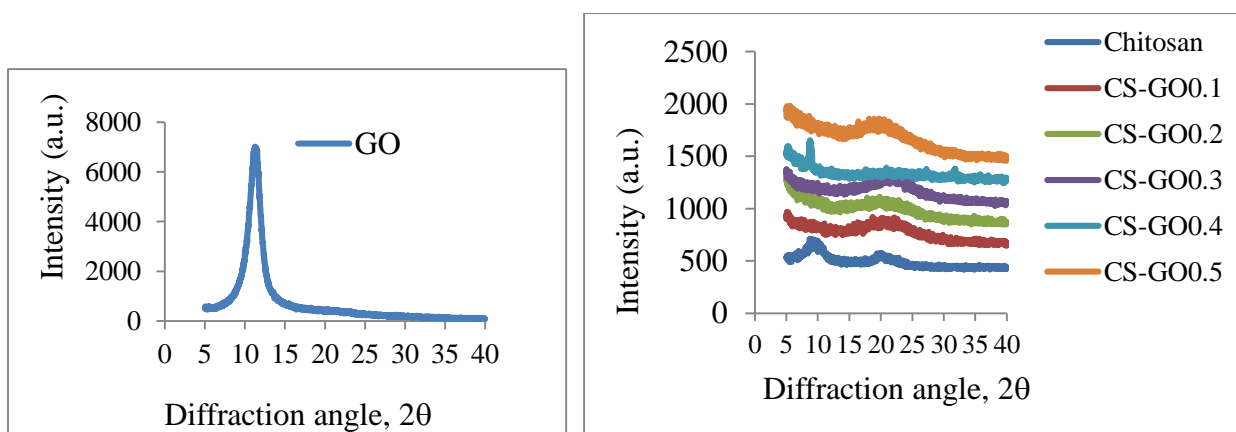


**Figure 5** XRD patterns of GO, CS and CSGO bionanocomposite

### FESEM-EDS Analysis

The surface morphology and the composition of the synthesized CS-GO nanocomposite samples have been investigated using field-emission scanning electron micrographs (FE-SEM) and the result for CSGO is displayed in Figure 6. The surfaces of CSGO particles with increased GO contents from 0.1 to 0.5 wt % became rough and porous (Figure 6 (a) to (e)). In particular, with an increase of the GO content in the CSGO particles, both the roughness and hole size of the particles increase. The FESEM images showed that bionanocomposite did not show porous structure because the pore sizes were gradually decreasing due to the percentage increase of graphene oxide



stocking on the polymer matrix, which also indicates development of strong hydrogen bond interactions between graphene oxide and polymer. To check the chemical composition of the material, an energy dispersive X-ray (EDX) spectroscopy analysis was also performed. Table 3 shows the elemental composition of CS-GO bionanocomposite samples, which confirms the presence of C, N and O ions in the matrix. The EDS results are also consistent with the weight percentage of C, N and O. From quantitative analysis it is evident that bionanocomposite samples contains approximately 60.68 % C, 3.37 % N and 35.95 % O by weight in CSGO0.1, 60.47 % C, 3.18 % N and 36.36 % O by weight in CSGO0.2, 64.57 % C, 1.85 % N and 33. 58 % O by weight in CSGO0.3, 47.88 % C, 3.75 % N and 48.37 % O by weight in CSGO0.4, and 61.38 % C, 1.94 % N and 36.68 % O by weight in CSGO0.5 respectively. These results were further found consistent with the XRD data.

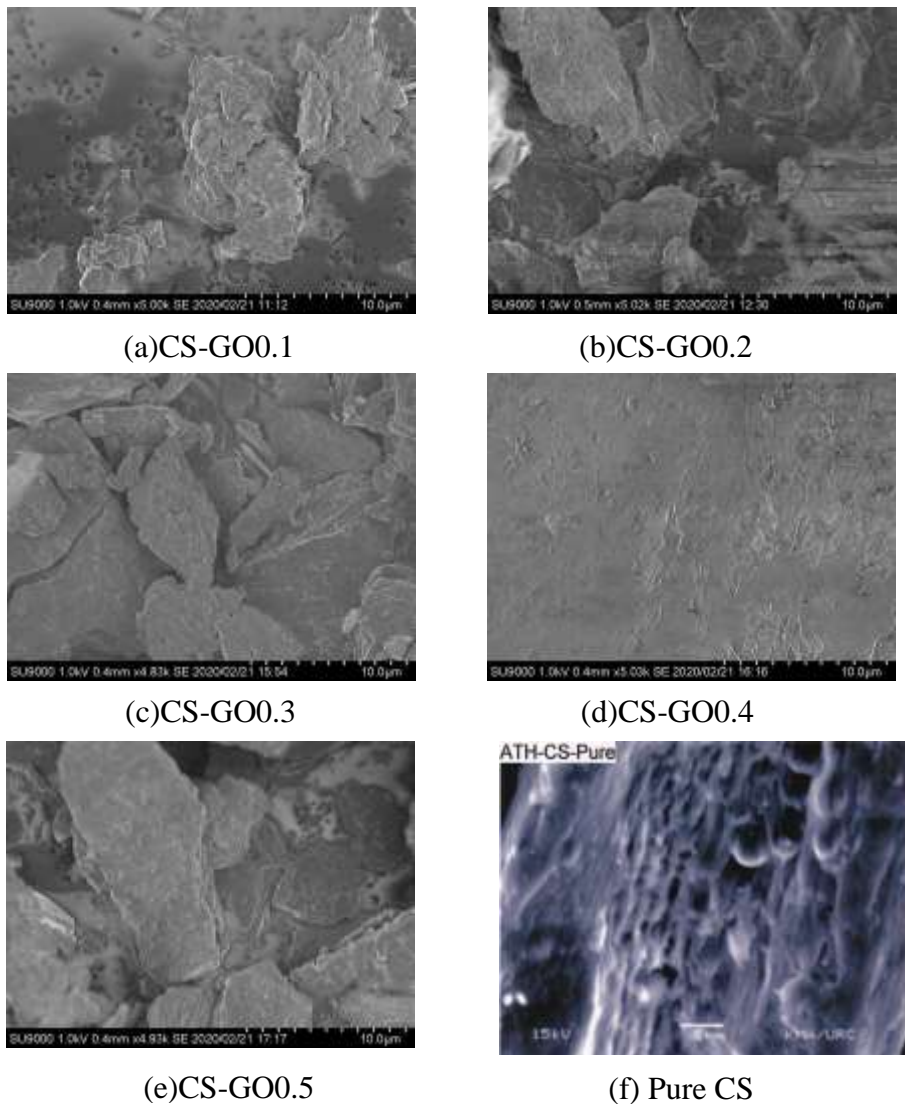


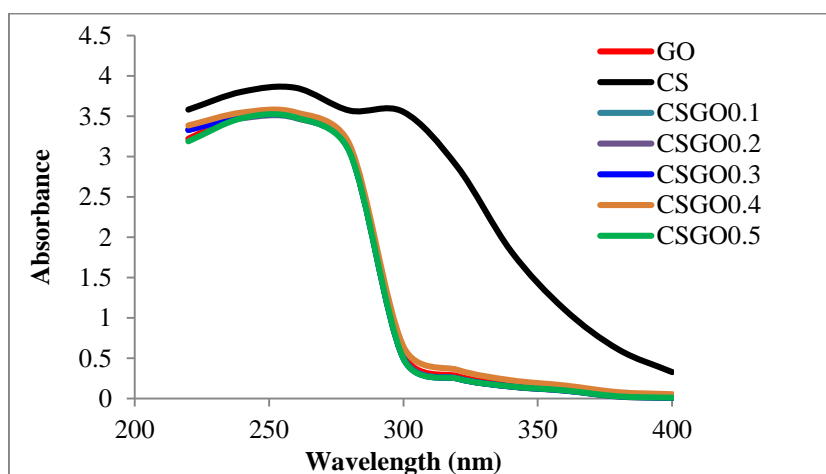
**Figure 6** SEM images of chitosan-graphene oxide bionanocomposite

**Table 2 Compositional analysis of the CS-GO by EDS**

Sample	Atomic % in composites		
	C	N	O
CS-GO0.1	60.68	3.37	35.95
CS-GO0.2	60.47	3.18	36.36
CS-GO0.3	64.57	1.85	33.58
CS-GO0.4	47.88	3.75	48.37
CS-GO0.5	61.38	1.94	36.68

### UV-vis absorption spectra

The UV-Vis spectra of the CSGO composite is shown in Figure 7. Pure GO shows the one absorption peaks at 240 nm due to the  $\pi$ - $\pi^*$  transition of C=C (Wong *et al.*, 2015; Xu *et al.*, 2013). Emadi *et al.* (2006) presented that the CS peaks are expected at 240 nm. After attachment with CS, the peaks of GO have shown a bathochromic shift. This shift in absorption maxima might be attributed to the formation of particles in the nano scale. This also indicates the strong covalent interaction between GO and CS where the active ester group of GO might have reacted with the amine groups on CS, forming an amide bond between GO and CS. (Suneetha, 2018).

**Figure 7** UV-vis spectra of GO and CSGO

### Particle Size Study of GO and CSGO by Dynamic Light Scattering

The size of the CSGO is controlled by the parameters influencing the colloidal stability, i.e., ionic strength, pH, charge on the particles, temperature, solvent viscosity, and dielectric constant of the solvent (Sun *et al.*, 2016). The particle size distribution of GO and CSGO nanocomposite were determined using Dynamic Light Scattering (DLS) (Figure 8 (a) to (f)). The average diameter of the GO is 496.7 nm. Due to that, the size is low; the GO do not overlap when dispersed in a solution allowing the construction of scaffolds without GO agglomerations (Valencia, 2018). The average diameter of the prepared CSGO nanocomposites are 999.1 nm for CSGO0.1, 881.1 nm for CSGO0.2, 627.6 nm for CSGO0.3, 628.8 nm for CSGO0.4 and 544.5 nm for CSGO0.5. It was found that the increasing the GO content, the lower will be the average diameter. Therefore, It can be observed that the average diameter of all of the prepared CSGO nanocomposite are higher than that of pure GO.

### Zeta Potential Measurement

The zeta potential is an important factor for characterizing the stability of colloidal dispersions and provides a measure of the magnitude and sign of the effective surface charge associated with the double layer around the colloid particle. Changes in the zeta potential in the presence of polymer may be caused by three different effects involving the following: the presence of the charges coming from the polymer dissociated functional groups in the by-surface layer of the solid, the shift of the slipping plane by the macromolecules adsorbed on the metal oxide surface, and the displacement of the counter-ions in the Stern layer as a result of the polymer adsorption (Vincent,1974).

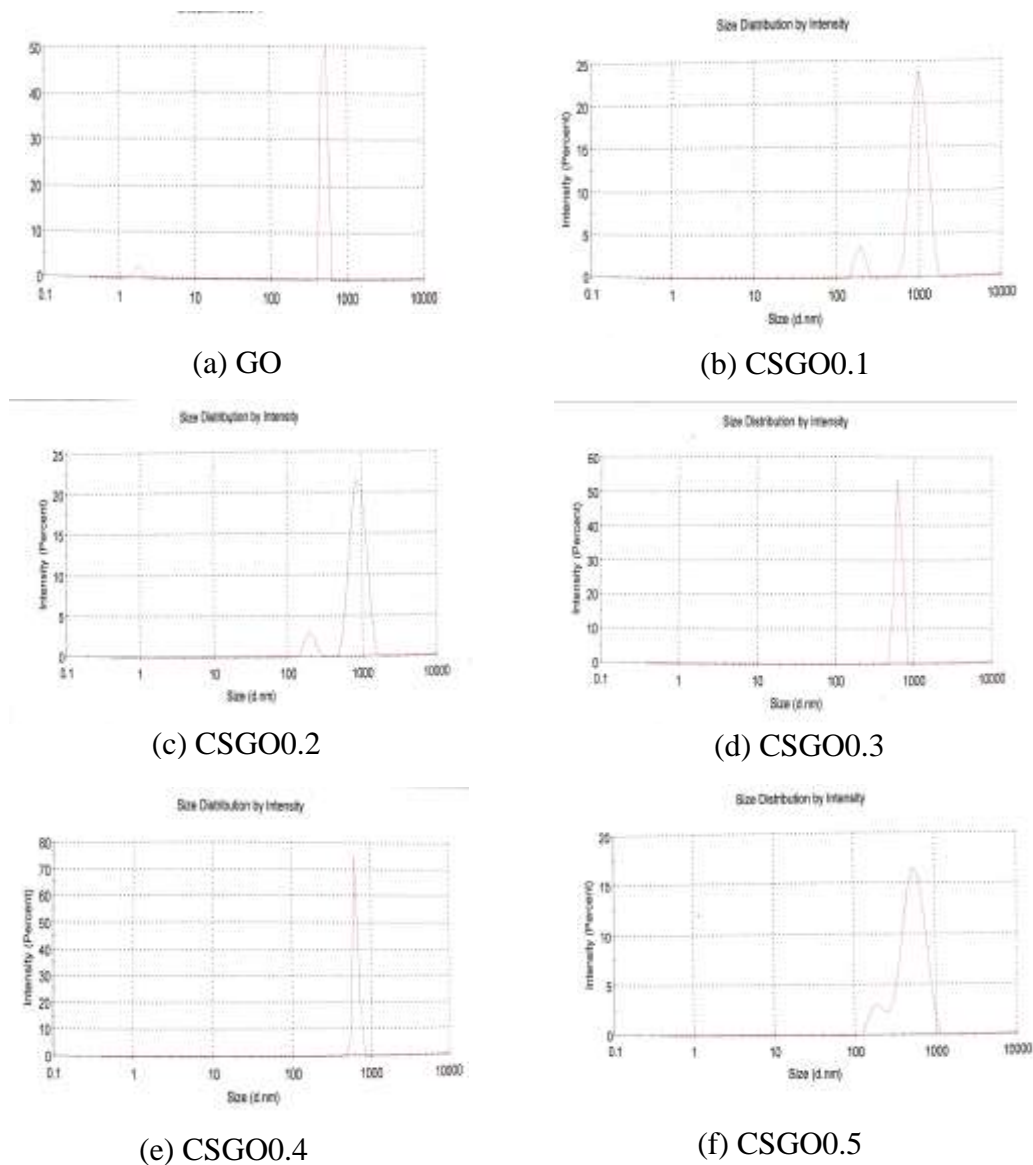


**Figure 8** DLS of particles of GO and CSGO nanocomposite

These effects occur simultaneously influencing the obtained zeta potential values. Reduction or increasing the potential is related to the fact which of the above mentioned phenomena predominates. The presence of the dissociated functional groups results in the zeta potential changes depending on the ionic nature of polyelectrolyte; negatively charged groups (e.g., carboxylic groups) cause decrease of  $\zeta$ , whereas the positively charged groups (e.g., amino groups) contribute to the increase in the zeta potential value. The adsorbed polymer macromolecules are

responsible for the decrease of the zeta potential connected with the shift of the slipping plane from the solid surface. The influence of the counter-ion displacement effect on the zeta potential is more complex and depends on the experiment conditions especially the charge of the colloidal particles (Ostolska, 2014).

The zeta potentials of the obtained pure GO and CSGO in distilled water (pH=7.4) are also showed in Figure 9 and Table 3. As seen in Table 3, the zeta potential and calculated average diameter of the obtained GO and CSGO is suitable range because can be used to evaluate the stability of colloidal systems, zeta potential is very important parameters which reflect their potential as carrier of ultrasound imaging contrast agents, which needs to be inert thus easy to trace and remove during in-vivo using process. It is well known that higher absolute value of zeta potential means higher stable state of colloidal systems, and potential values higher than +30 mV or lower than -30 mV permits a basically stable suspension (Sun *et al.*, 2016).

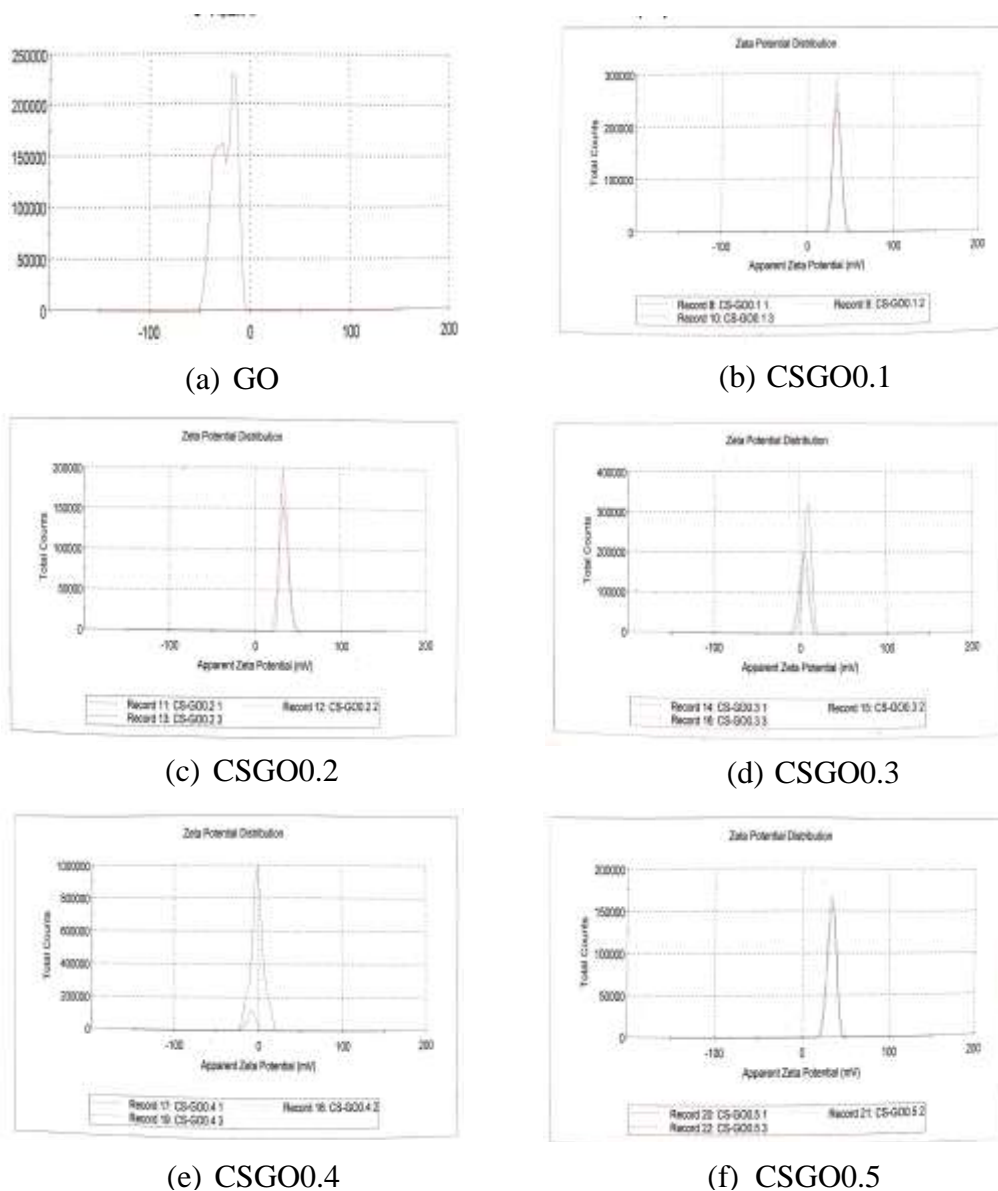


**Figure 9** zetapotential measurement of GO and CSGO nanocomposite

**Table 3 The zeta potential and calculated average diameter of the GO and CSGO**

Sample	Zeta potential (mV)	Average diameter calculated by laser particle size (nm)
GO	- 25.0	249.2
CSGO0.1	+ 33.9	594.6
CSGO0.2	+ 34.1	538.7
CSGO0.3	+ 2.73	627.6
CSGO0.4	-1.38	628.8
CSGO0.5	+ 32.8	369.8

Furthermore, zeta potential data reflect the stability of colloidal systems of the GO and CSGO nanocomposite dispersed in water. The zeta potential values of the GO and CSGO are listed in Table 3. As seen in table, the zeta potential value of pure GO is  $- 25$  mV. All the CSGO nanocomposite except CSGO0.4 obtained show a favorable positive zeta potential value. So, it was found that the zeta potential values of the CSGO increased when particle size increased than that of pure GO due to the amino group related boarded electric double layer surrounding GO. The amide groups act as neutral functional groups to maintain and strengthen the negative charges on the surface of GO, which was the key factor for dispersibility of GO in water. According to DLS results, the advantages for GO reveal their usefulness for size determination in aqueous media for studies related to biological applications, sensing and toxicity.

### Conclusion

The biocompatible and biodegradable chitosan based graphene oxide bionanocomposites were prepared by solvent casting method and confirmed by FT IR, TG-DTA, XRD, FE-SEM and UV-vis. The FT IR spectrum suggested that interactions existed between CS and GO as evidenced by the downshift of the C=O stretching vibration of the amide group at  $1620.24\text{ cm}^{-1}$ . The thermal studies showed that the loading level of the graphene oxide can affect the decomposition temperature of the bionanocomposites. Optical microscope shows that pure GO and CSGO bionanocomposites have a higher quantity of aggregates with fewer fine particles around the large aggregates in 5 MP. FE SEM micrograph of the nanocomposite showed the presence of the biopolymer chitosan with its porous, rough, granular morphology, the GO with its flat multilayer structure and all of CSGO with rough surface morphology with porous structure. The UV-vis absorption showed optical properties. The bionanoparticles size and surface charge were measured by dynamic light scattering spectroscopy and zeta potential analyzer. According to the results, the synthesized CSGO showed the dispersion peaks, at 594.6 nm with + 33.9 mV in CSGO0.1, at 538.7 nm with + 34.1 mV in CSGO0.2, at 627.6 nm with + 2.73 mV, at 628.8 nm with  $- 1.38$  mV in CSGO0.4 and at 369.8 nm with + 32.8 mV in CSGO0.5, respectively. All the results demonstrated that graphene oxide was well-dispersed in the chitosan matrix, and there are the strong H-bondings between hydroxy groups of the chitosan and hydroxy groups of the graphene oxide. The main contribution of the present work is that the synthesis of chitosan based graphene oxide bionanocomposite may be used for waste water pollution and tissue regeneration.

### Author Information

\*Corresponding Author: E-mail: ninithan@uy.edu.mm

### ORCID

Aung Than Htwe, <http://orcid.org/0000-0002-2937-8117>

## Acknowledgements

The authors would like to thank the Department of Higher Education, Ministry of Education and University of Yangon for some support to do this research. This research was supported by the KAPLAT program (JSPS Core-to-Core) Japan and Osaka University for intensive 2020. We would like to acknowledge KAPLAT Program Coordinator Professor Dr Hideaki OHGAKI, Institute of Advanced Energy, Kyoto University. Finally, We are also thankful to Nanotechnology Open Facility, Osaka University, for providing zetasizer, XRD, and FESEM facilities.

## References

- Aung Than Htwe. (2018). "Environmentally Effective Biodegradable and Antimicrobial Properties of Biowaste Chitosan-Polyvinyl Alcohol Hydrogel Composite Film", *International Journal of Scientific and Engineering Research*, vol. 9 (9), pp. 928-934.
- Bissessur, R., Liu, P. K. Y., White, W., and Scully, S. F. (2006). "Encapsulation of Polyanilines into Graphite Oxide", *Langmuir*, vol. 22(4), pp. 1729–1734.
- Emadi, F., Amini, A., Gholami, A., and Ghasemi Y. (2017). "Functionalized Graphene Oxide with Chitosan for Protein Nanocarriers to Protect Against Enzymatic Cleavage and Retain Collagenase Activity", *Sci. Rep.*, vol. 7(42258), pp. 1-13.
- Han, D., Yan, L., Chen, W., and Li, W. (2011). "Preparation of Chitosan/Graphene Oxide Composite Film with Enhanced Mechanical Strength in the Wet State", *Carbohydrate Polymers*, vol. 83, pp. 653–658.
- Kausar, A. (2019). "Polymer and Modified Chitosan-Based Nanocomposite: Impending Material for Technical Application", *Polymer-Plastics Technology and Materials*, vol. 158771, pp.1-15.
- Konwar, A., Kalita, S., Kotoky, J., and Chowdhury, D. (2016). "Chitosan–Iron Oxide Coated Graphene Oxide Nanocomposite Hydrogel: A Robust and Soft Antimicrobial Biofilm", *ACS Appl. Mater. Interfaces*, vol. 8, pp. 20625–20634.
- Kumara, S., Koha, J. (2014). "Physiochemical and Optical Properties of Chitosan Based Graphene Oxide Bionanocomposite", *International Journal of Biological Macromolecules*, vol. 70, pp. 559–564.
- Nath, J., Chowdhury, A., and Dolui, S. K. (2018). "Chitosan/Graphene Oxide-Based Multifunctional pH-Responsive Hydrogel with Significant Mechanical Strength, Self-Healing Property, and Shape Memory Effect", *Adv Polym Technol.*, vol. 37, pp. 3665-3679.
- Ostolska, I., and Wisniewska, M. (2014). "Application of the Zeta Potential Measurements to Explanation of Colloidal Cr<sub>2</sub>O<sub>3</sub> Stability Mechanism in the Presence of the Ionic Polyamino Acids", *Colloid Polym Sci.*, vol. 292, pp. 2453-2464.
- Quilaqueo, M., Krumm, M. G., Figueroa, R. R., Troncoso, E., and Esta, H. (2019). "Determination of Size Distribution of Precipitation Aggregates Using Non-Invasive Microscopy and Semiautomated Image Processing and Analysis", *Minerals*, vol. 9 (724), pp. 1-14.
- Sun, D., Kang, S., Liu, C., Lu, Q., Cui, L., and Hu, B. (2016). "Effect of Zeta Potential and Particle Size on the Stability of SiO<sub>2</sub> Nanospheres as Carrier for Ultrasound Imaging Contrast Agents", *Int. J. Electrochem. Sci.*, vol. 11, pp. 8520 – 8529.
- Suneetha, R. B. (2018). "Spectral, Thermal and Morphological Characterization of Biodegradable Graphene Oxide-Chitosan Nanocomposites", *J. Nanosci. Tech.*, vol. 4(2), pp. 342-344.
- Tu, X. Y. F., Li, L., Shang, S., and Tao, X. (2010). "Well-Dispersed Chitosan/Graphene Oxide Nanocomposites", *ACS Applied Materials and Interfaces*, vol. 2(6), pp. 1707–1713.
- Valencia, C., Valencia, C. H., Zuluaga, F., Valencia, M. E., Mina, J. H., and Tovar, C. D. G. (2018). "Synthesis and Application of Scaffolds of Chitosan-Graphene Oxide by the Freeze-Drying Method for Tissue Regeneration", *Molecules*, vol. 23(2651), pp. 1-16.
- Vincent, B. (1974). "The Effect of Adsorber Polymers on Dispersion Stability", *Adv Colloid Interf.*, vol.4, pp.193-277.
- Wong, C. P. P., Lai, C. W., Lee, K. M., and Hamid, S. B. A. (2015). "Advanced Chemical Reduction of Reduced Graphene Oxide and Its Photocatalytic Activity in Degrading Reactive Black 5", *Sci. Tech. Adv. Mater.*, vol. 8, pp. 7118-7128.
- Wu, K., Liu, X., Li, Z., and Jiao, Y. (2020). "Fabrication of Chitosan/Graphene Oxide Composite Aerogel Microspheres with High Bilirubin Removal Performance", *Materials Science & Engineering*, vol. C 106(110162), pp. 1-10.
- Xu, S., Yong, L., and Wu, P. (2013). "One-pot, Green, Rapid Synthesis of Flowerlike Gold Nanoparticles/ Reduced Graphene Oxide Composite with Regenerated Silk Fibroin as Efficient Oxygen Reduction Electrocatalysts", *ACS Appl. Mater. Interf.*, vol. 5, pp. 654-662.
- Yang, X., Tu, Y., Li, L., Shang, S., and Tao, X. (2010). "Well-Dispersed Chitosan/Graphene Oxide Nanocomposites", *ACS Applied Materials & Interfaces*, vol. 2(6), pp. 1707-1713.